

PAPER

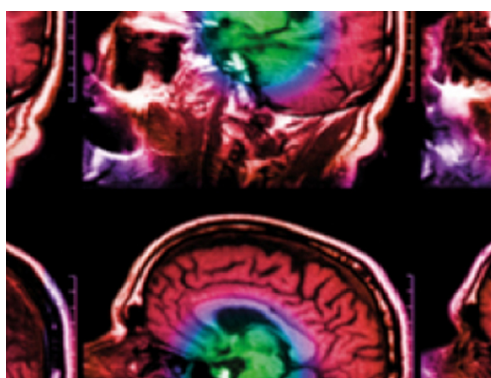
Sinus or not: a new beat detection algorithm based on a pulse morphology quality index to extract normal sinus rhythm beats from wrist-worn photoplethysmography recordings

Recent citations

- [Respiratory activity extracted from wrist-worn reflective photoplethysmography in a sleep-disordered population](#)
Gabriele B Papini *et al*

To cite this article: Gabriele B Papini *et al* 2018 *Physiol. Meas.* **39** 115007

View the [article online](#) for updates and enhancements.



IPEM | IOP

Series in Physics and Engineering in Medicine and Biology

Your publishing choice in medical physics,
biomedical engineering and related subjects.

Start exploring the collection—download the
first chapter of every title for free.



PAPER

Sinus or not: a new beat detection algorithm based on a pulse morphology quality index to extract normal sinus rhythm beats from wrist-worn photoplethysmography recordings

Gabriele B Papini^{1,2,3} , Pedro Fonseca^{1,2} , Linda M Eerikäinen^{1,2}, Sebastiaan Overeem^{1,3}, Jan W M Bergmans^{1,2} and Rik Vullings¹

¹ Department of Electrical Engineering, TU/e, Den Dolech 2, 5612 AZ Eindhoven, Netherlands

² Philips Research, High Tech Campus, 5656 AE Eindhoven, Netherlands

³ Kempenhaeghe Foundation, Sleep Medicine Centre, PO Box 61, 5590 AB Heeze, Netherlands

E-mail: g.papini@tue.nl

Keywords: quality index, arrhythmia, sinus rhythm, photoplethysmography, pulse rate variability, morphology

Abstract

Objective: Wrist-worn photoplethysmography (PPG) can enable free-living physiological monitoring of people during diverse activities, ranging from sleep to physical exercise. In many applications, it is important to remove the pulses not related to sinus rhythm beats from the PPG signal before using it as a cardiovascular descriptor. In this manuscript, we propose an algorithm to assess the morphology of the PPG signal in order to reject non-sinus rhythm pulses, such as artefacts or pulses related to arrhythmic beats. **Approach:** The algorithm segments the PPG signal into individual pulses and dynamically evaluates their morphological likelihood of being normal sinus rhythm pulses via a template-matching approach that accounts for the physiological variability of the signal. The normal sinus rhythm likelihood of each pulse is expressed as a quality index that can be employed to reject artefacts and pulses related to arrhythmic beats. **Main results:** Thresholding the pulse quality index enables near-perfect detection of normal sinus rhythm beats by rejecting most of the non-sinus rhythm pulses (positive predictive value 98%–99%), both in healthy subjects and arrhythmic patients. The rejection of arrhythmic beats is almost complete (sensitivity to arrhythmic beats 7%–3%), while the sensitivity to sinus rhythm beats is not compromised (96%–91%). **Significance:** The developed algorithm consistently detects normal sinus rhythm beats in a PPG signal by rejecting artefacts and, as a first of its kind, arrhythmic beats. This increases the reliability in the extraction of features which are adversely influenced by the presence of non-sinus pulses, whether related to inter-beat intervals or to pulse morphology, from wrist-worn PPG signals recorded in free-living conditions.

1. Introduction

1.1. Physiological monitoring with photoplethysmography

Over recent decades wearable devices for general consumer applications, such as fitness trackers and smartwatches, increasingly have been used in medical and diagnostic applications. The need for unobtrusive and inexpensive monitoring in certain areas of healthcare, such as cardiac and sleep monitoring, is an important driving force for the development of medically graded wearable devices and algorithms (Russo *et al* 2015, Eapen *et al* 2016, Piwek *et al* 2016). Photoplethysmography (PPG) is one of the most promising technologies for wearable medical monitoring (Allen 2007). A PPG sensor uses one or more LEDs to illuminate the skin and a photo-diode to measure the quantity of light that is either transmitted through (transmissive PPG) or reflected (reflective PPG) by the tissue. The acquired PPG signal describes the variation of blood volume in the micro-vessels that is caused by the pulsatile nature of the circulating blood. PPG technology has been researched broadly because it can be used to derive a substantial number of physiologically relevant signals and features, such as respiration and heart rate variability (HRV) (Allen 2007, Lázaro *et al* 2011, Charlton *et al* 2017). In turn, these

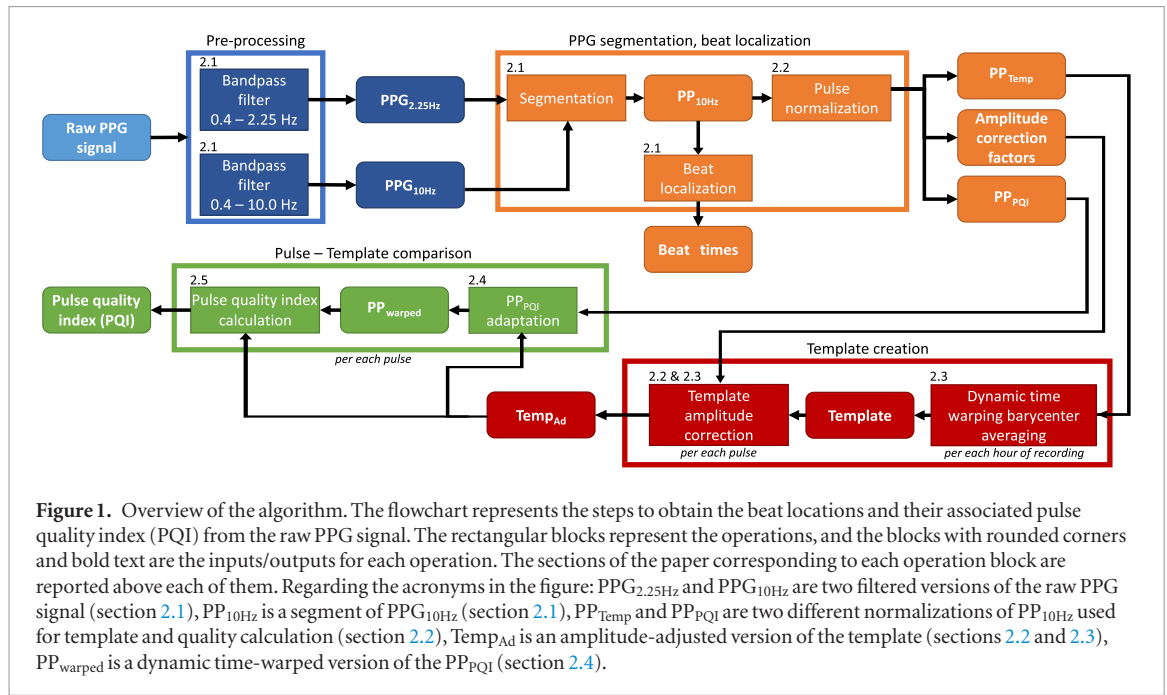
signals and features can be used to develop algorithms to monitor or classify various physiological phenomena. Reflective PPG is commonly applied in consumer devices, such as smartwatches, as it is easily embeddable in wrist-worn devices and enables continuous and relatively unobtrusive monitoring of cardio-circulatory activity. Several research studies have been conducted on wrist-worn PPG devices for medical applications with the intent to complement or replace more classical diagnostic techniques, such as polysomnography in sleep research and Holter ECG in cardiac monitoring (Bonomi *et al* 2016, Eerikainen *et al* 2017, Fonseca *et al* 2017).

For several applications, it is necessary to evaluate the quality and the regularity of the PPG signal in order to correctly extract the desired information. For instance, the removal of artefacts and arrhythmic beats from the inter-beat intervals (IBI) is paramount for computation of accurate HRV features. The irregularities caused by artefacts and non-sinus rhythm beats can increase IBI variability or bias IBI analysis and, therefore, corrupt HRV estimation (Camm *et al* 1996, Peltola 2012). In addition to their effect on HRV calculation, the presence of pulses from arrhythmic beats hampers the calculation of PPG-morphology-related features, such as PPG-derived respiration, due to the different hemodynamical response as compared to normal sinus rhythm beats (Camm *et al* 1996, Sološenko *et al* 2017). Signal quality assessment is particularly important for PPG because this signal is more prone to be corrupted when compared, for example, with an ECG signal. The PPG signal can be distorted by motion artefacts, low blood perfusion or sub-optimal contact between the sensor and the skin (Allen 2007, Schäfer and Vagedes 2013, Tamura *et al* 2014). At the same time, evaluating the quality of PPG is not a trivial task, as the morphology of the pulses is highly variable due to the broad spectrum of physiological parameters influencing the signal. The pulse morphology depends on the location of PPG measurement, the pressure applied to the sensor, the systemic and local blood pressure, cardiorespiratory dynamics, and factors influencing the mechanical properties of the vessels, such as arterial stiffness due to age or plaque buildup (Linder *et al* 2006, Allen 2007, Lázaro *et al* 2011, Tamura *et al* 2014, Hickey *et al* 2015). Moreover, the presence of pulses caused by arrhythmic beats such as premature ventricular contractions can be hidden by adjacent sinus rhythm pulses (Gil *et al* 2013, Sološenko *et al* 2017).

1.2. Quality assessment in PPG signals

Several algorithms for beat detection and quality assessment of PPG signals are described in the literature. Some of them estimate the quality of each pulse by thresholding specific morphological features, such as the duration of the rising slope and the amplitude of the PPG pulse (Sukor *et al* 2011, Fischer *et al* 2017). Furthermore, the thresholds for quality assessment are often defined heuristically or experimentally and are not necessarily valid for every PPG recording set-up. For example, some signal-amplitude-related thresholds require adjustment depending on the location or the type of PPG sensor (Allen 2007, Nijboer *et al* 1981). Other algorithms assess the quality of each PPG pulse by comparing it with a pulse template derived from the PPG signal itself. Such a template is often obtained by averaging multiple PPG pulses, and the quality is then calculated by directly comparing each individual pulse with the template, typically using one or more matching metrics such as the Pearson's correlation coefficient (Karlen *et al* 2012, Orphanidou *et al* 2015) or the dynamic time warping (DTW) distance (Li and Clifford 2012). Depending on the set of pulses considered, averaging the pulse signals can lead to a distorted template because of variability in the morphology of the pulses (Boudaoud *et al* 2005, Petitjean *et al* 2014). Moreover, direct comparison between a pulse and a template could lead to misclassification of a sinus rhythm pulse as a corrupted pulse, for instance when pulse morphology changes due to a postural change. In addition, metrics like the Pearson's correlation coefficient evaluate only the strength of the linear relationship between two variables. Therefore, it might not be sensitive to morphological changes that do not affect the rise-decline behavior of the PPG pulses, such as arrhythmic phenomena, but which are relevant to identify. We recently proposed an algorithm that overcomes these drawbacks (Papini *et al* 2017). This algorithm calculates the pulse quality by comparing each individual PPG pulse to a template obtained from a set of pulses via DTW-based averaging. The pulse-template comparison is mediated by the DTW of the pulse onto the template in order to account for the physiological variability of the PPG signal. However, the warping of the PPG pulse is not constrained and could therefore over-adapt the pulses to the template. This limits its applicability when a high similarity between the non-sinus rhythm pulse and the template is present, e.g. when the pulses are generated by arrhythmic beats. In addition, similar to the algorithms in the literature that we are aware of, this algorithm was developed and tested only on transmissive PPG, conventionally used in medical pulse oximeters. Moreover, none of the algorithms presented in the literature are developed to reject arrhythmic pulses and most of them were not tested in the presence of arrhythmias or in long-term recordings in free-living conditions such as in overnight recordings. Therefore, questions remain regarding their applicability and reliability in important real-world applications such as night-by-night sleep analysis and patient follow-up after hospital discharge.

This paper describes an extended version of the algorithm presented previously (Papini *et al* 2017). Here we describe an algorithm to assess the quality of individual PPG pulses, defined as the likelihood of being generated by normal sinus rhythm contractions. The quality index is assessed by comparing PPG pulse morphology to an adaptive template. The template is created via DTW barycenter averaging of several (DBA) pulses in order to be



insensitive to physiological differences in the pulses used to create the template and to guarantee a tailored template for every recording. The comparison between each pulse and the template is mediated by constrained DTW in order to account for the physiological variability of pulse morphology during sinus rhythm. The performance of the algorithm to classify normal sinus rhythm beats is tested on two datasets containing overnight free-living data from a wrist-worn reflective PPG device and analyzed in terms of beat detection and rejection rate of pulses caused by arrhythmic beats.

2. Methods: pulse quality index estimation algorithm

Figure 1 illustrates an overview of the algorithm; each of the steps will be described in the following sections. Regarding the abbreviations used, the subscript indicates the main characteristic of an element (e.g. $Temp_{Ad}$ is the adapted template); PP indicates a pulse of a PPG signal (e.g. PP_{10Hz} is a pulse of PPG_{10Hz}); the abbreviations ending in s have to be considered plural (e.g. PPs_{10Hz} is the plural form of PP_{10Hz}).

2.1. PPG pre-processing, segmentation and beat localization

The raw PPG signal is filtered to obtain two versions with different frequency components:

- $PPG_{2.25Hz}$: a 3rd-order zero-phase band-pass Butterworth filter with cut-off frequencies of 0.4 Hz and 2.25 Hz is used to remove high-frequency components related to noise and to the diastolic peak and the low-frequency components related to respiration and body position changes (Allen 2007) (figure 2(a)). This enhances the two local minima defining the start and the end of each pulse. The local minima are found according to

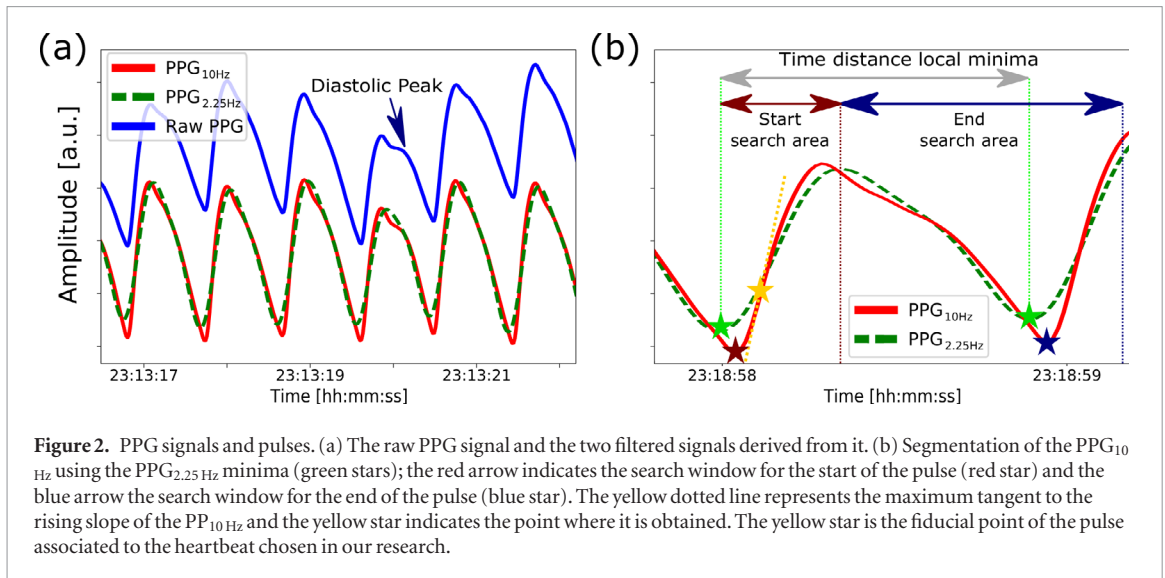
$$l = \{t \mid \text{sign } PPG_{2.25Hz}(t) \neq \text{sign } PPG_{2.25Hz}(t-1) \text{ \& } PPG_{2.25Hz}(t) > 0 \text{ \& } PPG_{2.25Hz}(t) < 0\}, \quad (1)$$

where $PPG_{2.25Hz}$ and $\dot{PPG}_{2.25Hz}$ indicate, respectively, the first and second derivative of $PPG_{2.25Hz}$.

- PPG_{10Hz} : a 3rd-order zero-phase band-pass Butterworth filter with cut-off frequencies of 0.4 Hz and 10 Hz is used to preserve the morphology of the PPG pulses which should still exhibit the component related to the diastolic peak (figure 2(a)). PPG_{10Hz} is segmented in PPs_{10Hz} using the local minima of $PPG_{2.25Hz}$ (figure 2(b)) according to the following equations:

$$l_i = i\text{th local minimum time}, \quad (2)$$

$$\text{peak} = \{t \mid PPG_{2.25Hz}(t) = \max PPG_{2.25Hz}(l_i, l_{i+1})\}, \quad (3)$$



$$\text{start} = \{t \mid \text{PPG}_{10 \text{ Hz}}(t) = \min \text{PPG}_{10 \text{ Hz}}(l_i, \text{peak})\}, \quad (4)$$

$$\text{end} = \{t \mid \text{PPG}_{10 \text{ Hz}}(t) = \min \text{PPG}_{10 \text{ Hz}}(\text{peak}, l_{i+1} + \frac{l_{i+1} - l_i}{4})\}, \quad (5)$$

$$\text{PP}_{10 \text{ Hz}} = \text{PPG}_{10 \text{ Hz}}(\text{start}, \text{end}). \quad (6)$$

The resulting $\text{PP}_{10 \text{ Hz}}$ that have a duration above 1.5 s or below 0.5 s, corresponding to a heart rate outside normal sinus rhythm range of 40–120 beats per minute (bpm), are excluded from further analysis. The exclusion criteria are slightly broader than the normal resting HR range in adults (40–90 bpm) in order to retain HR changes that may be caused by conditions unrelated to cardiovascular conditions, such as obstructive sleep apnea (Penzel *et al* 2003, Mason *et al* 2007). The remaining $\text{PP}_{10 \text{ Hz}}$ are upsampled to 1 kHz (in case recorded with a lower sampling frequency) using a cubic spline interpolation in order to localize more accurately their key points, such as their peaks. This procedure is commonly employed for ECG signals in order to better define the beat time location in the QRS complexes (Ellis *et al* 2015). Since each PPG pulse is the hemodynamic consequence of a cardiac contraction, it is possible to associate a fiducial point of the pulse with a heartbeat. The algorithm detects the largest first derivative in the rising slope of $\text{PP}_{10 \text{ Hz}}$ as the fiducial point (yellow star in figure 2(b)) since we found it to reproduce accurately the ECG-derived IBI (Nano *et al* 2017).

2.2. Pulse normalization

The amplitude of the PPG pulses can vary significantly during a recording due, for instance, to a change in body position or to different pressure applied to the sensor (Linder *et al* 2006, Tamura *et al* 2014). Therefore, it is necessary to normalize the $\text{PP}_{10 \text{ Hz}}$ amplitude before creating a pulse template out of an ensemble of pulses. The normalized version of $\text{PP}_{10 \text{ Hz}}$ is calculated according to

$$\text{amplitude} = |\max \text{PP}_{10 \text{ Hz}} - \min \text{PP}_{10 \text{ Hz}}|, \quad (7)$$

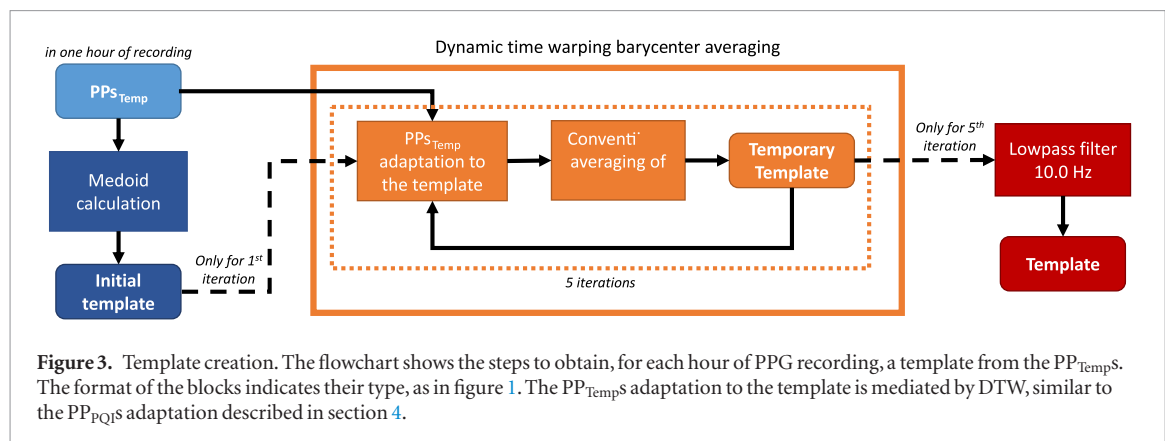
$$\text{shift} = (\max \text{PP}_{10 \text{ Hz}} + \min \text{PP}_{10 \text{ Hz}})/2, \quad (8)$$

$$\text{PP}_{\text{Temp}} = \frac{\text{PP}_{10 \text{ Hz}} - \text{shift}}{\text{amplitude}}. \quad (9)$$

Sudden substantial increases of the $\text{PP}_{10 \text{ Hz}}$ amplitudes are often representative of signal corruption. In these cases, the amplitude information is helpful in identifying segments that should have a low quality index. For this reason, a second normalized version of the $\text{PP}_{10 \text{ Hz}}$, which is used for quality index calculation, is computed as

$$\text{PP}_{\text{PQI}} = \text{PP}_{10 \text{ Hz}} - \text{shift}. \quad (10)$$

The different normalization approaches complicate the estimation of the similarity between the template derived from the PP_{Temp} and each PP_{PQI} because the first represents a normalized amplitude while the second contains a varying amplitude. Therefore, in order to be able to compare template and PP_{PQI} , it is necessary to adjust the template amplitude with a correction factor before each comparison between the template and PP_{PQI} . To derive the correction factors, a time series comprising all the amplitudes obtained in (7) is stored. First, the algorithm removes from the amplitude time series all elements that have a value 50% higher or lower than the previous or the

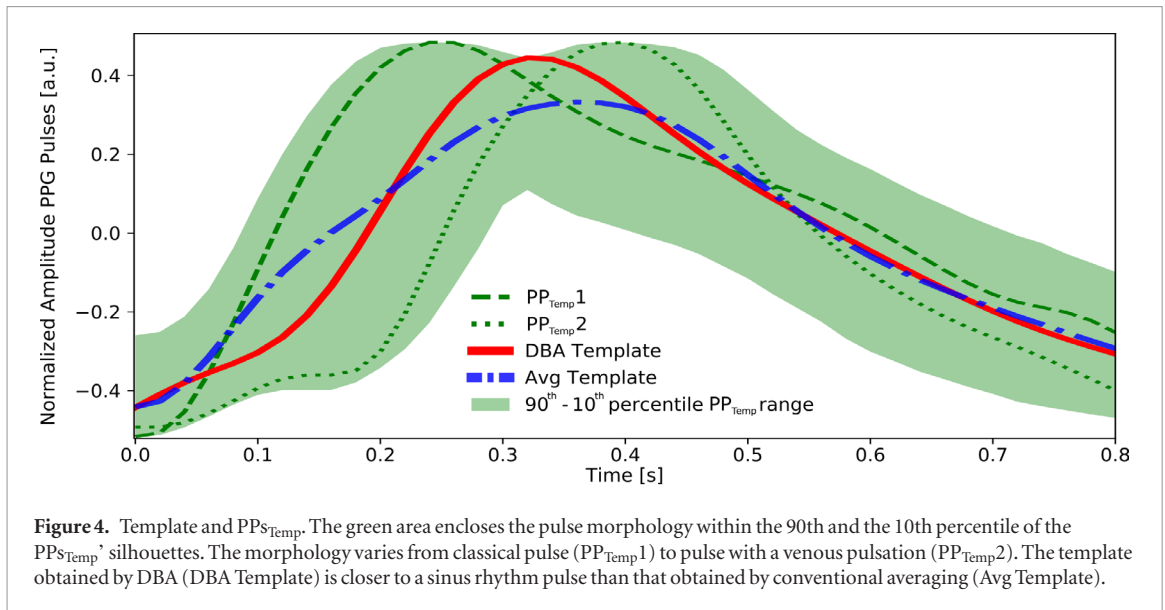


following value. Then the clipped amplitude time series is interpolated at 4 Hz using a cubic spline interpolation and filtered with a 3rd-order zero-phase low-pass Butterworth filter with a cut-off frequency of 1.5 Hz. The cut-off frequency is chosen to confidently include physiological amplitude variations since these are not expected to occur faster than the respiration frequency (a frequency range from 4 to 60 breaths per minute, i.e. from 0.067 Hz to 1 Hz, was considered) (Charlton *et al* 2017). Finally, the filtered signal is resampled at the same time locations of the original amplitude time series. In this way, the algorithm suppresses abnormal amplitude variations from each PP_{PQI} while retaining the low-frequency physiological amplitude variations. The cleaned amplitude time series is used as a series of correction factors; the adjusted templates ($Temp_{AdS}$) are obtained by multiplying the template by the corresponding correction factors for each comparison with the PP_{PQI} .

2.3. Template creation

The literature describes several examples of template extraction from cardiovascular signals such as ECG and ballistocardiogram for the purpose of beat classification and signal quality estimation (Clifford 2002, Redmond *et al* 2012, Brüser *et al* 2013, Orphanidou *et al* 2015). In our algorithm, the quality assessment of each PPG pulse is also based on a template-matching approach: each PP_{PQI} is compared with an amplitude-adjusted template describing the morphology of an uncorrupted and regular PPG pulse, i.e. a pulse free from movement artefacts and caused by a normal sinus rhythm beat. The pulses in a PPG signal are a clear example of a time series that changes in shape: the pulse morphology changes according to normal physiological variation, such as heart rate (HR), vascular tone and body position (Linder *et al* 2006, Allen 2007). For this reason, our algorithm calculates the pulse template by means of DBA (Petitjean *et al* 2014). This allows the time series to be averaged by iteratively decreasing the DTW distance between an initial template and each individual pulse (figure 3). In each iteration, the resulting averaged time series is used as the initial template for the next iteration. The DBA is initialized with the medoid of the PP_{Temp} as initial template, and this initial template is refined during five iterations (Petitjean *et al* 2014). The number of iterations is chosen empirically to ensure the computation of a pulse template with a correct morphological representation of the pulses, in an efficient computation time. The resulting pulse template is filtered using a 3rd-order low-pass Butterworth filter with a cut-off frequency of 10 Hz to remove high-frequency components introduced by the DBA. This guarantees that the template has the same frequency components as the PPG segments used to obtain it (PP_{Temp}) and of the PPG segments used to calculate the quality index (PP_{PQI}). A separate template is calculated for each one-hour segment of the PPG recording. The choice of one hour segments represents a compromise between a sufficient amount of uncorrupted pulses while keeping computational time within reasonable limits. However, the algorithm is also able to handle shorter segments, for instance of eight minutes, as described in Papini *et al* (2017).

Figure 4 illustrates an example where DBA outperforms a conventional averaging procedure. In this case, the subset of pulses used has a varying morphology caused by the presence of a venous pulsation at the beginning of some of the PPG pulses (e.g. in PP_{Temp} 2) (Shelley *et al* 1993). The morphological variety is remarkably broad (the area highlighted in green) and conventional averaging does not yield a pulse rising slope characteristic of an actual PPG pulse. Instead, the DBA maintains the overall shape of the PPG pulses and, in addition, includes the influence of the venous pulsation. Aligning the pulses before conventional averaging would improve the results, but would also require removal of the part of the PPG pulses related to the venous pulsation and, therefore, part of the physiological information present in the signal. In our algorithm, it is not necessary to account separately for the pulse misalignment because the DBA accounts for it (pulse adaptation step in figure 3). Thanks to this, the DBA can operate on segments with different lengths, eliminating the need to zero-pad or trim segments to a fixed length before aligning and finally averaging them.



2.4. PP_{PQI} adaptation

The proposed algorithm uses DTW to derive PP_{warped} from the warping of PP_{PQI} to the template calculated for the one hour of PPG signal they belong to (figure 5). In contrast with our previous algorithm (Papini *et al* 2017), we now apply two constraints to the DTW in order to avoid a distortedly warped PP_{PQI} (Sakoe and Chiba 1978). One constraint limits the maximum time warping to 0.3 s and the other limits the number of matching points to a maximum of 3. The first constraint is derived heuristically and corresponds approximately to two times the standard deviation of the inter-pulse intervals in our datasets. The second constraint is chosen in order to be able to transform a PP_{PQI} from 0.5 s to 1.5 s, and vice versa, and to guarantee a balanced warping to each point of the pulses. In this way, the entire spectrum of pulses, with a duration within the boundaries set in the PPG signal segmentation, can be covered. Finally, the PP_{warped} are filtered using the same approach as for the template in order to remove high-frequency components introduced by the DTW (figure 5) and to enable the comparison with the $Temp_{Ad}$ to calculate the PQI.

2.5. PQI calculation

The DTW produces a warped pulse that matches best, within the constraints, with the derived pulse template. However, some differences between them remain, for two reasons: first of all, because the DTW modifies the time locations of each point, but not their values, and second, because of the DTW constraints used. In this way, part of the morphological discrepancies between PP_{PQI} and $Temp_{Ad}$ remain in the PP_{warped} . These residual differences are used by the algorithm to calculate the quality index (PQI) of each PPG pulse. An overview of the procedure is shown in figure 6 and the details are explained in the following equations.

First, the algorithm finds the indices of each sample of PP_{warped} with a difference higher than 10% with respect to the corresponding samples of the $Temp_{Ad}$ (11):

$$UP = \left\{ i \in \mathbb{Z}^+ \mid \left| \frac{PP_{warped}(i) - Temp_{Ad}(i)}{Temp_{Ad}(i)} \right| > 0.1 \right\} \quad (11)$$

where \mathbb{Z}^+ denotes the set of positive integers ranging from one to the number of samples of PP_{warped} . These indices allow the classification of each point of PP_{warped} as unmatched (UP) or matched (MP) to the relative $Temp_{Ad}$ points. The 10% threshold is chosen heuristically and lower threshold values appear not to drastically influence the algorithm's performance. Instead, thresholds above 20% are not recommended in order to avoid decreasing the ability to correctly calculate the PQI. By using a 10% threshold, the algorithm can account for small deviations that the DTW cannot fully compensate for, and can treat them as residual physiological variations. The quantity of unmatched and matched points, respectively N_{UP} and N_{MP} , are used to calculate the percentage of matching points as

$$N_{MP\%} = N_{MP} / (N_{MP} + N_{UP}). \quad (12)$$

The second step consists in calculating the root mean square error of the unmatched points in respect to $Temp_{Ad}$ according to

$$RMSE_{UP} = \begin{cases} 0 & \text{if } N_{UP} = 0 \\ \sqrt{\frac{\sum_{j=1}^{N_{UP}} [Temp_{Ad}(UP_j) - PP_{warped}(UP_j)]^2}{N_{UP}}} & \text{if otherwise.} \end{cases} \quad (13)$$

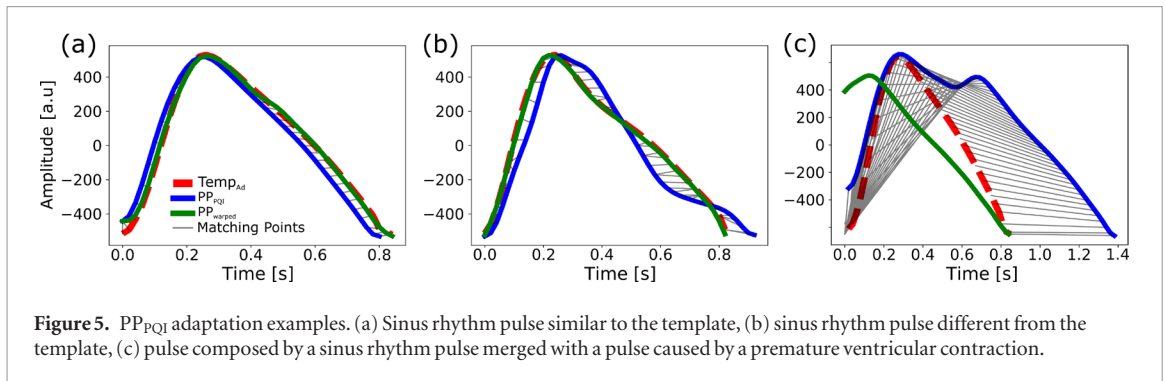


Figure 5. PP_{PQI} adaptation examples. (a) Sinus rhythm pulse similar to the template, (b) sinus rhythm pulse different from the template, (c) pulse composed by a sinus rhythm pulse merged with a pulse caused by a premature ventricular contraction.

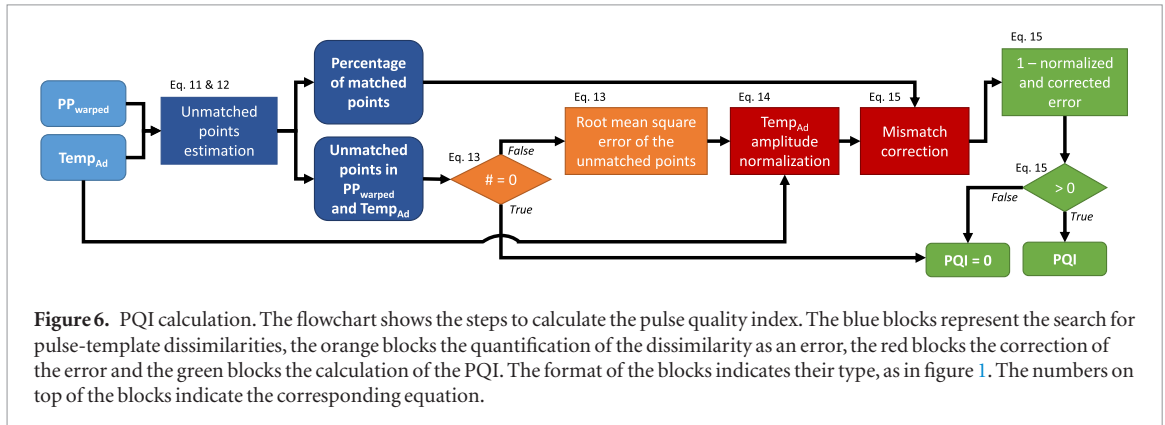


Figure 6. PQI calculation. The flowchart shows the steps to calculate the pulse quality index. The blue blocks represent the search for pulse-template dissimilarities, the orange blocks the quantification of the dissimilarity as an error, the red blocks the correction of the error and the green blocks the calculation of the PQI. The format of the blocks indicates their type, as in figure 1. The numbers on top of the blocks indicate the corresponding equation.

The $RMSE_{UP}$ represents the pulse-template dissimilarity, but it depends on the amplitude of $Temp_{Ad}$, which varies for each PP_{warped} - $Temp_{Ad}$ comparison. In fact when N_{UP} is not zero, the higher the amplitude of $Temp_{Ad}$, the higher the $RMSE_{UP}$ is, regardless of the actual dissimilarity between $Temp_{Ad}$ and PP_{warped} . Therefore, the algorithm normalizes the $RMSE_{UP}$ for the amplitude of $Temp_{Ad}$:

$$RMSE_{norm} = RMSE_{UP} / (\max(Temp_{Ad}) - \min(Temp_{Ad})). \quad (14)$$

In the case where the error is larger than the amplitude of $Temp_{Ad}$, the PP_{warped} certainly has a poor quality, therefore its PQI is set to zero. The $RMSE_{norm}$ has the disadvantage that it takes into account only the magnitude of the mismatch and not the number of the mismatching points. This characteristic negatively influences the PQI because it makes PQI insensitive to situations where there is a high number of unmatched points (low $N_{MP\%}$) in combination with a low $RMSE_{norm}$. The algorithm accounts for this by dividing the $RMSE_{norm}$ by $N_{MP\%}$. This ratio can be higher than 1, resulting in a negative PQI. Since there is no reason to have a PQI lower than zero, the PQI is set to 0 in case the ratio is larger than 1, i.e. the $RMSE_{norm}$ is larger than $N_{MP\%}$:

$$PQI = \max \{0, 1 - RMSE_{norm} / N_{MP\%}\}. \quad (15)$$

The algorithm calculates a single PQI varying from 0—low quality, highly corrupted or highly influenced by arrhythmia—to 1—high quality, uncorrupted and belonging to normal sinus rhythm—for each pulse in a one-hour segment of the PPG recording.

In cases where the average of the non-null PQIs is below 0.9 in a one-hour segment of the recording, the PQI is considered invalid, the algorithm excludes the pulses with the 20% lowest PQI, recalculates the template and reassesses the quality of all pulses in that segment. If the PQI is still not valid, the template calculated in the previous hour of the recording is used. In cases where there is no template available, a PQI of zero is assigned to all the pulses in the segment.

3. Materials and validation methods

3.1. Datasets

Two datasets were used to assess the performance of the PQI as a measure of normal sinus rhythm likelihood of a pulse. The first dataset (Heart Health Sleep dataset, HHS) consists of 26 overnight recordings from 16 healthy adults and is described by Fonseca *et al* (2017) as *Validation set 1*. The subjects in the HHS datasets did not have any previous history of cardiovascular disorders and the subjects were assumed to have normal sinus rhythm. The second dataset (Atrial Fibrillation dataset, AF) consists of 16 24h recordings from 16 patients, of which four had continuous atrial fibrillation, one atrial flutter and 11 sinus rhythm with premature contractions. This

dataset is described by Eerikainen *et al* (2017); for this research, only the overnight part of each recording is considered in order to have a stationary recording condition, as in most literature (Aboy *et al* 2005, Karlen *et al* 2012, Li and Clifford 2012, Fischer *et al* 2017). The start and end time in bed were annotated by a researcher by analyzing the accelerometer signal. The HHS and AF datasets contain ECG (respectively from lead II and 12-lead) and wrist-worn PPG signals recorded simultaneously. In addition, the ECG data in the AF dataset was visually analyzed by a clinical expert using an automated software to label every beat either as sinus rhythm, AF, premature atrial contraction, premature ventricular contraction, artefact, or unknown. For the HHS dataset, the beats in the ECG signal were automatically detected using a QRS detector and the post-processing localization algorithm described in Fonseca *et al* (2014). The ECG signals comprise 769 935 beats in the HHS dataset and 437 337 beats in the AF dataset. The AF dataset comprises 276 041 sinus rhythm beats and the arrhythmic beats comprise 9778 premature atrial contractions (PAC), 8060 premature ventricular contractions (PVC), 107 485 beats during atrial fibrillation (AFib), 35 873 beats during atrial flutter (AFlu) and 100 unknown/artefact. During the benchmarking of the algorithm, the unknown/artefact beats are treated in the same way as arrhythmic beats because of their limited amount and since both groups should anyway be rated with a low quality index.

3.2. Validation procedures

The current version of the algorithm differs from that described in Papini *et al* (2017) in the two constraints employed in the pulse adaptation (section 4). The constraints do not refer to specific pulse types (e.g. uncorrupted, arrhythmic or artefact) or to a specific pathology. Given the large number of beats used to validate the algorithm, and the independence of the constraints from arrhythmic/artefact influences on the pulse morphology, we are convinced that there is no risk of overfitting to the validation datasets. The algorithm is tested regarding sinus rhythm beat detection capability and rejection of arrhythmic beats. Its performance is evaluated in comparison with a reference: either manually or automatically annotated beats from the ECG signal. Moreover, the performance is compared with the correlation-derived PQI described in Clifford *et al* (2015) and summarized in the next section.

3.2.1. Correlation-derived pulse quality index

An algorithm to derive a PQI based on the Pearson's correlation coefficient between the PPG pulses and a template was publicly released during the PhysioNet/Computing in Cardiology Challenge of 2015. The algorithm takes as input a PPG signal in addition to the pulse segmentation points, and outputs a quality index for each pulse. The algorithm first computes a template from all the pulses and then uses this template to calculate the correlation-based PQI of the same pulses (PQI_{Corr}). In our research, the correlation-based algorithm takes as input the PPs_{Temp} and uses these pulses for template creation and quality assessment. The beat locations within the pulses are defined as in our algorithm, i.e. the point with the maximum slope in the rising part of the PPG pulse. The correlation-based algorithm uses a standard ensemble averaging to derive the template and resamples the pulses to match the number of samples of the template before calculating the quality index. The PQI_{Corr} is validated in the same way as the PQI, allowing us to benchmark the performance of our proposed algorithm with respect to a commonly used approach described in the literature.

3.2.2. Sinus rhythm beat detection

The algorithm described in this manuscript gives as an output the beat times and the PQI associated with each pulse. The performances of the beat detection algorithms are calculated by comparing the beat times derived from PPG to the annotated beat times from ECG, as in Karlen *et al* (2012) and Aboy *et al* (2005). Prior to the performance evaluation, the beat times derived from the PPG signal are synchronized with those derived from the ECG signal. This is done by maximizing the cross-correlation of the IBIs obtained from both signals (Fonseca *et al* 2017). Sensitivity and positive predictive values (SEN, PPV) are employed to quantify the beat detection rate of normal sinus rhythm beats (ANSI-AAMI 1998). In order to be able to compute these metrics, true detections are determined by defining a maximum time difference allowed between the reference beat from ECG and a detected beat from PPG, as in Aboy *et al* (2005), Karlen *et al* (2012) and Papini *et al* (2017). Every missed detection is considered a false negative while every detection not belonging to any detection window is considered a false positive. SEN and PPV are then calculated as

$$SEN = \frac{\text{True detections}}{\text{True detections} + \text{Missed detections}}, \quad (16)$$

$$PPV = \frac{\text{True detections}}{\text{True detections} + \text{Not belonging detections}}. \quad (17)$$

The detection window for ECG-PPG beat matching is set to 125 ms in order to account for the pulse transit time variations that can generate local time differences between PPG and ECG beats even after the global

synchronization step, e.g. due to body position change (Foo *et al* 2005). PQI is used to discard pulses with a PQI lower than a predefined threshold. SEN and PPV are calculated for different thresholds in order to determine the operating characteristics of the algorithm regarding detection of beats annotated as sinus rhythm with respect to the others, i.e. arrhythmic beats, artefacts or corrupted pulses. The assumption is that by increasing the quality index threshold the PPV should increase, because more erroneous detections, i.e. artefacts and non-sinus rhythm beats, will be rejected. SEN and PPV are not calculated for the subjects with continuous AFib and AFlu because they do not have any beats labeled as sinus rhythm and the number of true detections cannot be calculated.

3.2.3. Rejection of arrhythmic beats

Each arrhythmic beat in the AF dataset has a reference label of PAC, PVC, AFlu or AFib. The capability of the algorithm to assign a low quality index to each arrhythmic beat is tested as the sensitivity to each of these types of beats (SEN_{Arr}). SEN_{Arr} is calculated in the same way as the sensitivity to sinus rhythm beats by now using the arrhythmic beats as the positive class instead of sinus rhythm beats. The assumption is that by increasing the PQI threshold the number of arrhythmic beats rejected should increase, and consequently the SEN_{Arr} should decrease due to the lower arrhythmic beat detection (true positives). The presence of an arrhythmic beat can also influence the morphology of a previous PPG pulse by, for instance, deforming its diastolic phase (Gil *et al* 2013, Sološenko *et al* 2017). Therefore, we determine a subject-specific time threshold as the median of the time distances between each peak and the corresponding end of each pulse in the complete recording (to account for the subject variability of the PPG signal). If two PPG beats are closer in time than the subject-specific threshold, the same label as that assigned to the subsequent PPG beat is also assigned to the first one. Subjects with continuous AFib or AFlu do not have any beats labeled as sinus rhythm, therefore their SEN_{Arr} is calculated separately from the other arrhythmic subjects. The four AFib subjects are treated differently from the rest because no sinus rhythm is present and, therefore, it is not possible to assess deviations from sinus rhythm. The AFlu subject is also treated separately because one form of the pathology reduces the ventricular contraction variability, on the contrary to the other arrhythmias (Scholz *et al* 2014). The pulses during atrial flutter are extremely regular and are therefore not distinguishable by simple morphological comparison. By isolating subjects with AFib and AFlu, the sensitivity to arrhythmic beats can be calculated over the entire AF dataset without being biased by the different types of arrhythmic populations, i.e. continuous as in AFib and AFlu versus intermittent PAC and PVC. Nonetheless, for these five subjects, the sensitivity to arrhythmic beats is calculated separately for each pathology for the overall number of arrhythmic beats. In addition, the overall quality indices values are calculated to describe the algorithm's behavior for these two arrhythmia cases and to compare it with the average quality indices for premature contractions and sinus rhythm beats using the (Mann and Whitney 1947) test. For the recordings with premature contractions, SEN_{Arr} is calculated for the overall number of arrhythmic beats, as the average of each subject's SEN_{Arr} and for the overall number of PAC and PVC beats.

4. Results

4.1. Sinus rhythm beat detection

The PPV and SEN for detecting normal sinus rhythm beats in the HHS and AF datasets calculated for PQI and PQI_{Corr} thresholds ranging from 0.0 to 0.8 are reported in figure 7. For both pulse quality indices, increasing the threshold of beat rejection increases the positive predictive value at the expense of sensitivity. While the positive predictive value is comparable in both datasets, the sensitivity is lower in the HHS dataset. The beat detection algorithm performs well, also without thresholding the PQI; the positive predictive value with a PQI threshold of 0.0 is around 97% and 95% in the HHS and the AF datasets, respectively. By increasing the PQI threshold, the positive predictive value increases consistently by around 2% and 3% in the two datasets with a moderate decrease in sensitivity. For a PQI threshold of 0.6, nearly all the beats are successfully matched with the reference beats from the ECG.

4.2. Arrhythmic beat rejection

The overall quality index distributions are reported in table 1. The beats belonging to the subjects with continuous Afib and Aflu have, respectively, significantly lower and higher quality indices compared to sinus rhythm beats. In table 2 the SEN_{Arr} is reported for the same quality index thresholds as used in the normal sinus rhythm beat detection performance evaluation. For each quality index threshold, the SEN_{Arr} is lower for the PQI when compared with the PQI_{Corr} , independently of how the metric is evaluated.

5. Discussion

In this paper, we describe and evaluate an algorithm to detect normal sinus rhythm beats from PPG signals by means of a pulse-quality-based rejection of arrhythmic beats and corrupted pulses. With respect to the detection

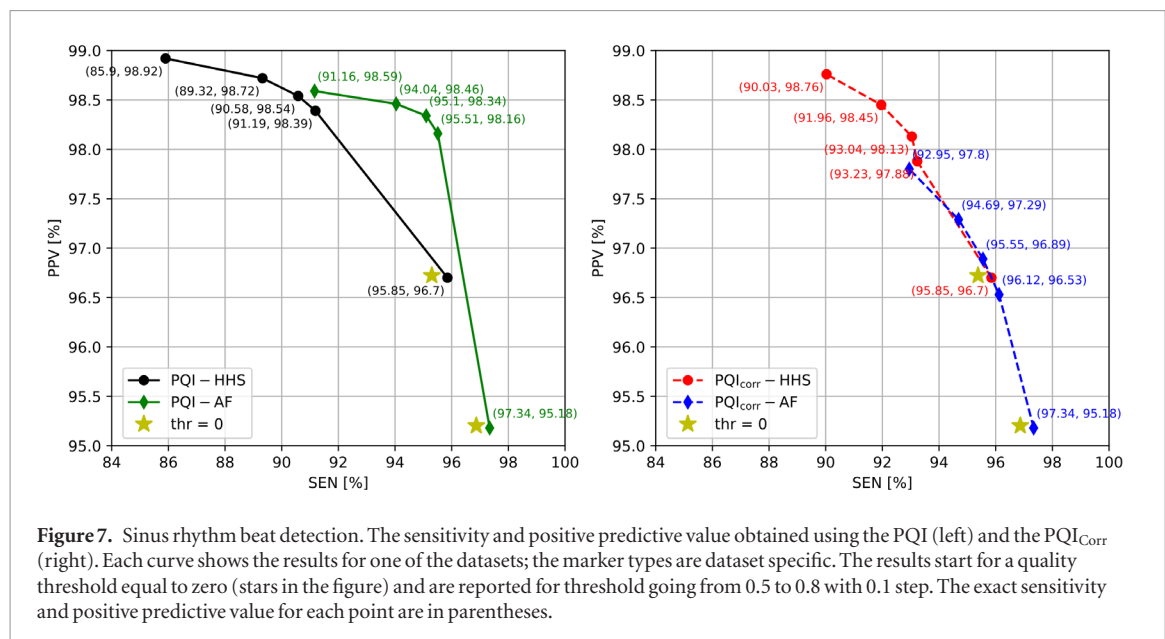


Table 1. Distribution of PQI and PQI_{corr} for each beat type.

	AFib	AFlu	PAC + PVC	Sinus rhythm
PQI avg \pm std	0.55 \pm 0.38 ^a	0.98 \pm 0.11 ^b	0.20 \pm 0.28 ^a	0.95 \pm 0.14
PQI _{corr} avg \pm std	0.68 \pm 0.26 ^a	0.98 \pm 0.08 ^b	0.57 \pm 0.29 ^a	0.95 \pm 0.10

Note. Statistically significantly lower (^a)/higher (^b) than Sinus rhythm beats ($p < 0.01$).

of normal sinus rhythm beats, the PQI calculated by comparing the PPG pulses and the signal specific templates achieves a performance which is on par with the literature. Using a threshold to reject beats based on the PQI leads to a good agreement with beats obtained from ECG, which is a more noise-resilient signal compared to the PPG signal for beat detection.

The sensitivity to sinus rhythm beats we obtained is lower compared to our previous work and to results reported in the literature (Aboy *et al* 2005, Karlen *et al* 2012, Fischer *et al* 2017, Papini *et al* 2017). However, this can be attributed to the datasets used for validation. An artefact present in the PPG signal is often not visible in the ECG signal, because the latter is less influenced by movement artefacts and because the PPG sensor often temporarily loses contact with the sensed area. For instance, limb-worn devices are more subject to body movements than the thorax or abdomen, where ECG is conventionally mounted. In addition, the lack of sinus rhythm annotation and the completely automatic detection of the reference beats make the HHS dataset sub-optimal to test the sinus rhythm detection capabilities of our algorithm. The annotation methodology of the HHS dataset can cause the inclusion of some artefacts of the ECG signal or arrhythmic beats as sinus rhythm beats. However, it is legitimate to assume that the large majority of the beats detected in the ECG signals of the HHS dataset are sinus rhythm beats because the dataset consists of healthy subjects, with no primary history of cardiovascular disorders or using any substance that could have influenced the cardiovascular activity (Fonseca *et al* 2017). In addition, the ECG beat detector has been published with good results and used in other research works (Radha *et al* 2017, Fonseca *et al* 2018). Nevertheless, the results obtained on the HHS dataset should not be considered on their own, but only as further evidence of the algorithm's performance besides what was obtained on the correctly annotated AF dataset. Despite this apparent decrease in performance, it should be emphasized that, unlike earlier work, this research focused on free-living recordings of healthy subjects and of patients with cardiac arrhythmias. The recording conditions introduce a higher physiological variability in the PPG signals due to the long recording duration and to the unconstrained set-up. Moreover, the number and different pathologies of the measured subjects enriches the morphological variability of the PPG signal. The reference used and the type of recordings contribute to a lower sensitivity to sinus rhythm beats, but the algorithm is able to provide—even for higher PQI thresholds—an average sensitivity higher than 90% together with positive predictive values close to 99%. In terms of sinus rhythm beat detection, the PQI performance is comparable to what is obtained using the PQI_{corr}. However, the positive predictive value is consistently higher for the PQI, especially for the AF dataset. This performance difference can be attributed to a higher specificity in assessing the quality of the arrhythmic beats: the PPG pulses associated with arrhythmic beats are more distinguishable and, hence, easier to reject when

Table 2. SEN_{Arr} (%) for the overall number of beats, per-subject average (avg \pm std) and overall number of beats for arrhythmia cases for different thresholds (Thr).

	Thr	0.0	0.5	0.6	0.7	0.8
PQI	Overall	46.92	6.90	4.90	3.75	2.65
	Per-subject	53.64 \pm 25.54	13.73 \pm 11.74	11.38 \pm 10.66	9.53 \pm 8.93	4.06 \pm 4.56
	PAC	62.43	11.00	7.92	6.16	4.40
	PVC	28.24	1.97	1.25	0.84	0.55
	AFib	80.70	55.88	51.80	44.06	30.68
	AFlu	98.40	97.34	97.13	96.78	95.78
PQI _{Corr}	Overall	46.92	30.03	25.10	19.62	12.53
	Per-subject	53.64 \pm 25.54	35.99 \pm 22.10	31.89 \pm 22.63	29.05 \pm 22.63	25.77 \pm 22.48
	PAC	62.43	39.69	33.50	25.95	15.74
	PVC	28.24	18.40	14.98	11.99	8.66
	AFib	80.70	63.47	56.91	48.34	36.45
	AFlu	98.40	97.90	97.70	97.50	97.16

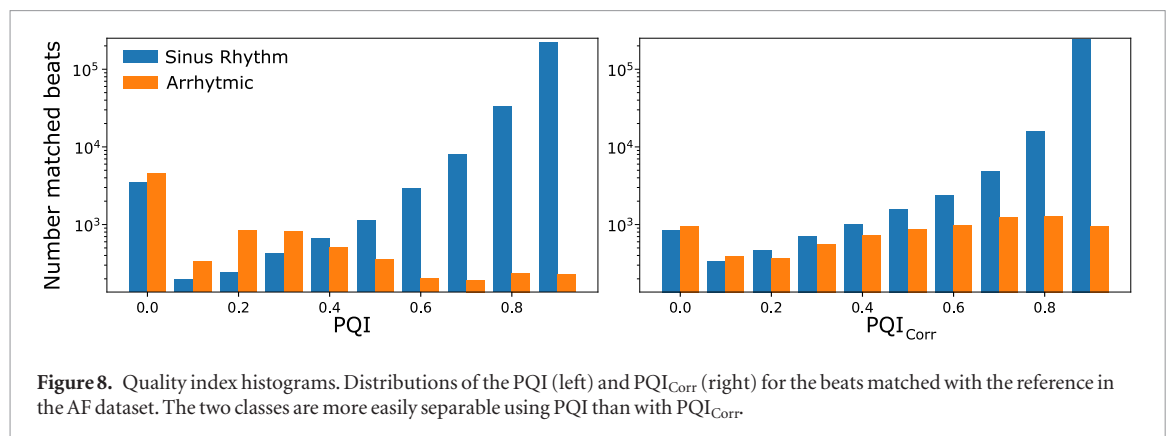
rated with PQI than with PQI_{Corr}. In fact, nearly all the arrhythmic beats are rated with a PQI below 0.6 while PQI_{Corr} distribution has the same trend for arrhythmic and sinus rhythm beats (figure 8).

The higher class separability between sinus rhythm and arrhythmic pulses using the PQI is reflected in the arrhythmic beat rejection results. The PQI is able, as desired, to decrease the overall sensitivity to arrhythmic beats—specifically to PACs and PVCs—to below 7% while with the PQI_{Corr} the SEN_{Arr} reaches 12% for a threshold of 0.8, i.e. close to the quality index suitable for sinus rhythm beats. Furthermore, this means that in order to have a proportion of arrhythmic beats lower than 12% using PQI_{Corr} one would have to sacrifice the sensitivity to sinus rhythm beats, making the SEN-SEN_{Arr} trade-off more disadvantageous than for PQI. In fact, PQI is able to guarantee, for every threshold, a lower presence of arrhythmic beats while maintaining a higher sensitivity to sinus rhythm beats. An example of the higher discriminative capacity of PQI can be seen in figure 5. The comparison between PP_{PQI} and the template in figure 5(c) by means of the Pearson's correlation coefficient overestimates the pulse quality by assigning a PQI_{Corr} of 0.89—indicating high similarity with the template—even though it is derived from the merging of a sinus rhythm PPG pulse with a premature ventricular contraction. Instead, the PQI correctly assigns a low quality index value to most similar pulse cases (in this example PQI is zero). Changing the similarity metric to a more sensitive one, such as the pulse-template distance derived via classical DTW (Li and Clifford 2012), can resolve the pulse quality overestimation, but at the same time it might increase the chance of underestimating the quality of uncorrupted pulses. For instance, in figure 5(b) the difference between the pulse and the template is not due to signal corruption or abnormal HR behavior, but the DTW distance increases by 20% with respect to figure 5(a), where the difference between template and pulse is almost absent.

The SEN_{Arr} of the PQI is better than that for PQI_{Corr} when calculated across all beats as well as when calculated per subject. In fact, the PQI offers a per-subject SEN_{Arr} three times lower with a twice as low standard deviation compared to the PQI_{Corr} indicating a lower between-subject variability of the results. This does not only guarantee a higher rejection of arrhythmic beats in each subject, but also a higher consistency in the results, suggesting a higher generalizability of the PQI approach. Moreover, the SEN_{Arr} of PQI is similar among the two arrhythmic conditions under evaluation, i.e. PAC and PVC, while the PQI_{Corr} tends to have a larger difference in performance.

The rejection of arrhythmic beats is higher when the recordings are mainly characterized by PVCs rather than PACs. This can be explained by the morphological differences in the PPG signal for pulses generated by the PVC and PAC beats. A pulse related to a PVC often tends to be merged with the sinus rhythm pulse that precedes it, resulting in a single PP_{PQI} (e.g. figure 5(c)). This occurs less frequently in the case of PACs. In fact, in the PVC recordings, 99% of the beats preceding the actual PVC beats were assigned a PVC label as compared to only 55% of PAC beats. The PP_{PQI} resulting from the merging of a sinus rhythm and PVC related pulses have a morphology that is significantly different than the generated templates and, therefore, are easier to correctly classify as low-quality pulses.

One of the limitations of the PQI is the inability to properly assess the normal sinus rhythm likelihood of every single beat/pulse in case an arrhythmic condition is continuously present in the PPG recording. However, in case of AFib the PQI is significantly lower than the PQI obtained for the sinus rhythm beats. This means that also when no normal sinus rhythm pulses are present, the algorithm can quantify the irregularity of the recording and assign a lower PQI to most of the pulses. This measure can, therefore, be used to exclude a subject completely from further analysis in case a PPG recording presents an overall low average PQI. The algorithm needs to be developed further to achieve a similar rejection rate during AFib as with PAC and PVC. One future development will be to separate the template creation from the PP_{Temp} in case of overall low average PQI in order to increase



the morphological difference between the arrhythmic pulses and the template. These expedients cannot be used in case of atrial flutter since this condition produces a significant reduction in contraction variability, which leads to pulses with an extremely regular morphology, as confirmed by an $AF_{Flu} SEN_{Arr}$ higher than the SEN for every threshold (table 2). In fact, the PQI distribution of beats from the AFlu subject is significantly higher than the PQI for any other cardiac condition and sinus rhythm pulsations. Even though the PQI cannot be used to flag the potential presence of a condition in the case of AFlu, it behaves as expected: regular pulses are classified with a higher quality index. To correct for this drawback, a standard 24 h Holter ECG monitoring could be used to confirm the suspicion of an atrial flutter.

Naturally, if arrhythmic beats or pulses are excluded when aiming to exclude pulses corrupted by movement artefacts, the resulting time series is not usable for arrhythmia detection. However, the information in the PQI can be used as an additional indicator for arrhythmia detection or to pre-select pulses deviating from the sinus rhythm.

Another limitation of our algorithm is that it is not suitable for on-line, real-time assessment of PPG pulse quality. However, by changing, for instance, the number of pulses required to derive the template, it could be adapted for such an application, with a trade-off between assessment delay (due to template build-up) and the power of the PQI in discriminating sinus rhythm and arrhythmic or corrupted beats.

6. Conclusion

We present a new beat detection algorithm for wrist-worn PPG signals. The algorithm allows the precise identification of normal sinus rhythm beats in a PPG signal recorded by a wrist-worn device. This is achieved by segmenting the signal into individual pulses and dynamically evaluating their quality via a template comparison approach. The algorithm can be employed to obtain inter-beat intervals or PPG pulse series comprised only of normal sinus rhythm beats by excluding artefacts and pulses corrupted by external or arrhythmic phenomena, and hence enabling, for instance, the calculation of HRV features or PPG-derived respiration. Moreover, the PQI can be used according to the application needs: for instance, a higher quality threshold can be used when analyzing the morphology of the PPG pulse; instead, a lower threshold can be set in cases of beat detection where the sporadic inclusion of a wrong beat can be corrected during post-processing of inter-beat intervals.

Future work on the algorithm will focus on a more application-specific PQI calculation, for instance by weighing the mismatch error according to its location on the PPG pulse. This could help to increase the sensitivity to sinus rhythm beats in the cases where, for example, only the rising slope of the PPG pulse is necessary for feature extraction.

Acknowledgments

This research was supported by STW/IWT in the context of the OSA + project (No. 14619). GBP would like to thank X L Aubert for contributing to the algorithm's development. The authors would like to express their gratitude to L Dekker and his team at the Catharina Hospital for help with collecting the patient data.

ORCID iDs

Gabriele B Papini <https://orcid.org/0000-0002-5752-9226>

Pedro Fonseca <https://orcid.org/0000-0003-2932-6402>

References

- Aboy M, McNamers J, Thong T, Tsunami D, Ellenby M S and Goldstein B 2005 An automatic beat detection algorithm for pressure signals *IEEE Trans. Biomed. Eng.* **52** 1662–70
- Allen J 2007 Photoplethysmography and its application in clinical physiological measurement *Physiol. Meas.* **28** R1
- ANSI-AAMI 1998 ANSI/AAMI EC57: testing and reporting performance results of cardiac rhythm and ST segment measurement algorithm
- Bonomi A G, Schipper F, Eerikainen L M, Margarito J, Aarts R M, Babaeizadeh S, de Morree H M and Dekker L 2016 Atrial fibrillation detection using photo-plethysmography and acceleration data at the wrist *Computing in Cardiology Conf.* pp 277–80
- Boudaoud S, Rix H and Meste O 2005 Integral shape averaging and structural average estimation: a comparative study *IEEE Trans. Signal Process.* **53** 3644–50
- Brüser C, Winter S and Leonhardt S 2013 Robust inter-beat interval estimation in cardiac vibration signals *Physiol. Meas.* **34** 123
- Camm A J et al 1996 Heart rate variability: standards of measurement, physiological interpretation and clinical use *Circulation* **93** 1043–65
- Charlton P H, Bonnici T, Tarassenko L, Alastruey J, Clifton D A, Beale R and Watkinson P J 2017 Extraction of respiratory signals from the electrocardiogram and photoplethysmogram: technical and physiological determinants *Physiol. Meas.* **38** 669
- Clifford G D 2002 Signal processing methods for heart rate variability *PhD Thesis* Department of Engineering Science, University of Oxford
- Clifford G D, Silva I, Moody B, Li Q, Kella D, Shahin A, Kooistra T, Perry D and Mark R G 2015 The PhysioNet/Computing in Cardiology Challenge 2015: reducing false arrhythmia alarms in the ICU *Computing in Cardiology Conf.* pp 273–6
- Eapen Z J, Turakhia M P, McConnell M V, Graham G, Dunn P, Tiner C, Rich C, Harrington R A, Peterson E D and Wayte P 2016 Defining a mobile health roadmap for cardiovascular health and disease *J. Am. Heart Assoc.* **5** e003119
- Eerikainen L M, Dekker L, Bonomi A, Vullings R, Schipper F, Margarito J, de Morree H and Aarts R 2017 Validating features for atrial fibrillation detection from photoplethysmogram under hospital and free-living conditions *Computing in Cardiology Conf.* pp 1–4
- Ellis R J, Zhu B, Koenig J, Thayer J F and Wang Y 2015 A careful look at ECG sampling frequency and R-peak interpolation on short-term measures of heart rate variability *Physiol. Meas.* **36** 1827
- Fischer C, Dömer B, Wibmer T and Penzel T 2017 An algorithm for real-time pulse waveform segmentation and artifact detection in photoplethysmograms *IEEE J. Biomed. Health Inform.* **21** 372–81
- Fonseca P, Aarts R M, Foussier J and Long X 2014 A novel low-complexity post-processing algorithm for precise QRS localization *SpringerPlus* **3** 376
- Fonseca P, den Teuling N, Long X and Aarts R M 2018 A comparison of probabilistic classifiers for sleep stage classification *Physiol. Meas.* **39** 055001
- Fonseca P, Weyssen T, Golema M S, Møst E I, Radha M, Lunsingh Scheurleer C, van den Heuvel L and Aarts R M 2017 Validation of photoplethysmography-based sleep staging compared with polysomnography in healthy middle-aged adults *Sleep* **40** zsx097
- Foo J Y A, Wilson S J, Williams G R, Harris M A and Cooper D M 2005 Pulse transit time changes observed with different limb positions *Physiol. Meas.* **26** 1093
- Gil E, Laguna P, Martínez J P, Barquero-Pérez Ó, García-Alberola A and Sörnmo L 2013 Heart rate turbulence analysis based on photoplethysmography *IEEE Trans. Biomed. Eng.* **60** 3149–55
- Hickey M, Phillips J P and Kyriacou P A 2015 The effect of vascular changes on the photoplethysmographic signal at different hand elevations *Physiol. Meas.* **36** 425
- Karlen W, Kobayashi K, Ansermino J M and Dumont G A 2012 Photoplethysmogram signal quality estimation using repeated Gaussian filters and cross-correlation *Physiol. Meas.* **33** 1617
- Lázaro J, Gil E, Bailón R and Laguna P 2011 Deriving respiration from the pulse photoplethysmographic signal *Computing in Cardiology* pp 713–6
- Li Q and Clifford G D 2012 Dynamic time warping and machine learning for signal quality assessment of pulsatile signals *Physiol. Meas.* **33** 1491
- Linder S, Wendelken S, Wei E and McGrath S 2006 Using the morphology of photoplethysmogram peaks to detect changes in posture *J. Clin. Monit. Comput.* **20** 151–8
- Mann H B and Whitney D R 1947 On a test of whether one of two random variables is stochastically larger than the other *Ann. Math. Stat.* **18** 50–60
- Mason J W, Ramseth D J, Chanter D O, Moon T E, Goodman D B and Mendzelevski B 2007 Electrocardiographic reference ranges derived from 79 743 ambulatory subjects *J. Electrocardiol.* **40** 228–34
- Nano M, Papini G, Fonseca P, Vullings R, Overeem S, Bergmans J and Aarts R 2017 Comparing inter beat and inter pulse intervals from ECG and PPG signals during sleep *Poster Session Presented at 11th Biomedica Summit (Eindhoven, Netherlands, Eindhoven, Netherlands, 9–10 May 2017)*
- Nijboer J A, Dorlas J C and Mahieu H F 1981 Photoelectric plethysmography-some fundamental aspects of the reflection and transmission methods *Clin. Phys. Physiol. Meas.* **2** 205
- Orphanidou C, Bonnici T, Charlton P, Clifton D, Vallance D and Tarassenko L 2015 Signal-quality indices for the electrocardiogram and photoplethysmogram: Derivation and applications to wireless monitoring *IEEE J. Biomed. Health Inform.* **19** 832–8
- Papini G B, Fonseca P, Aubert X L, Overeem S, Bergmans J W M and Vullings R 2017 Photoplethysmography beat detection and pulse morphology quality assessment for signal reliability estimation *39th Annual Int. Conf. of the IEEE Engineering in Medicine and Biology Society*
- Peltola M 2012 Role of editing of R–R intervals in the analysis of heart rate variability *Frontiers Physiol.* **3** 148
- Penzel T, Kantelhardt J W, Grote L, Peter J H and Bunde A 2003 Comparison of detrended fluctuation analysis and spectral analysis for heart rate variability in sleep and sleep apnea *IEEE Trans. Biomed. Eng.* **50** 1143–51
- Petitjean F, Forestier G, Webb G I, Nicholson A E, Chen Y and Keogh E 2014 Dynamic time warping averaging of time series allows faster and more accurate classification *IEEE Int. Conf. on Data Mining*
- Piwek L, Ellis D A, Andrews S and Joinson A 2016 The rise of consumer health wearables: promises and barriers *PLoS Med.* **13** 1–9
- Radha M, Zhang G, Gelissen J, de Groot K, Haakma R and Aarts R M 2017 Arterial path selection to measure pulse wave velocity as a surrogate marker of blood pressure *Biomed. Phys. Eng. Express* **3** 015022
- Redmond S J, Xie Y, Chang D, Basilakis J and Lovell N H 2012 Electrocardiogram signal quality measures for unsupervised telehealth environments *Physiol. Meas.* **33** 1517
- Russo K, Goparaju B and Bianchi M T 2015 Consumer sleep monitors: is there a baby in the bathwater? *Nat. Sci. Sleep* **7** 147
- Sakoe H and Chiba S 1978 Dynamic programming algorithm optimization for spoken word recognition *IEEE Trans. Acoust. Speech Signal Process.* **26** 43–9

- Schäfer A and Vagedes J 2013 How accurate is pulse rate variability as an estimate of heart rate variability?: a review on studies comparing photoplethysmographic technology with an electrocardiogram *Int. J. Cardiol.* **166** 15–29
- Scholz E P, Kehrle F, Vossel S, Hess A, Zitron E, Katus H A and Sager S 2014 Discriminating atrial flutter from atrial fibrillation using a multilevel model of atrioventricular conduction *Heart Rhythm* **11** 877–84
- Shelley K H, Dickstein M and Shulman S M 1993 The detection of peripheral venous pulsation using the pulse oximeter as a plethysmograph *J. Clin. Monit.* **9** 283–7
- Sološenko A, Petrénas A, Marozas V and Sörnmo L 2017 Modeling of the photoplethysmogram during atrial fibrillation *Comput. Biol. Med.* **81** 130–8
- Sukor J A, Redmond S J and Lovell N H 2011 Signal quality measures for pulse oximetry through waveform morphology analysis *Physiol. Meas.* **32** 369
- Tamura T, Maeda Y, Sekine M and Yoshida M 2014 Wearable photoplethysmographic sensors past and present *Electronics* **3** 282–302